Histology-Specific Radiotherapy Target Volume Delineation for NSCLC Based on Distinct Lymph Node Metastasis Patterns of Adenocarcinoma and Squamous Cell Carcinoma

Zheng Liu
General Hospital of Western Theater Command
Xiaomei Qian
General Hospital of Western Theater Command
Zhihui Li
General Hospital of Western Theater Command
Zhiming Chen
The 944th Hospital of PLA Joint Logistics Support Force
Guangjie Wang
General Hospital of Western Theater Command
Feifan Sun
General Hospital of Western Theater Command
Hui Gao
General Hospital of Western Theater Command
Jingjing Peng
General Hospital of Western Theater Command
Xiaoli Huang
General Hospital of Western Theater Command
Jianqiong Feng
General Hospital of Western Theater Command
Min Du
General Hospital of Western Theater Command
Jing Xian
General Hospital of Western Theater Command
Lingbo Bao
General Hospital of Western Theater Command
Hong Luo
General Hospital of Western Theater Command
BinLin Tang
General Hospital of Western Theater Command

Yiyang Hu
General Hospital of Western Theater Command
Yi Li
920th Hospital of Joint Logistics Support Force
Chao Wang
General Hospital of Western Theater Command
Chaoyang Jiang
General Hospital of Western Theater Command
Daijun Zhou
General Hospital of Western Theater Command
Dong Li
13438078785@163.com

General Hospital of Western Theater Command

Research Article

Keywords: Lung Adenocarcinoma (LUAD), Lung Squamous Cell Carcinoma (LUSC), Lymph Node Metastasis Pattern, PET/CT, Pathology, Radiotherapy Target Volume

Posted Date: January 28th, 2026

DOI: https://doi.org/10.21203/rs.3.rs-8318884/v1

Additional Declarations: No competing interests reported.

Abstract

Background

This study sought to characterize distinct regional lymph node metastasis (LNM) patterns of lung adenocarcinoma (LUAD) and squamous cell carcinoma (LUSC) using PET-CT imaging and postoperative pathology, and to provide evidence-based guidance for precise radiotherapy target volume delineation in NSCLC.

Methods

We retrospectively analyzed 422 PET-CT scans (281 LUAD, 141 LUSC) and 305 surgical pathology reports (236 LUAD, 69 LUSC) from our institution. Inter-group comparisons were performed using chi-square or Fisher's exact tests. Binary logistic regression models were utilized for multivariate analyses.

Results

PET-CT and pathological data exhibited high concordance in LNM distribution. Compared with LUSC, LUAD displayed more aggressive LNM behavior, with significantly higher metastasis rates to supraclavicular, contralateral mediastinal, and contralateral hilar nodes. In contrast, LUSC showed increased level 8 LNM, especially in left inferior lobe origin. Multivariate analysis revealed: LUAD with mediastinal invasion, ipsilateral multi-lobar nodules, or LNM at levels 2L/2R/3a/6 had higher 1L/1R metastasis risk; left inferior lobe origin or larger tumor diameter in LUSC hinted level 8 metastasis. Significant inter-nodal metastatic correlations were identified across different levels.

Conclusion

LUAD and LUSC exhibit distinct histology- and subsite-specific LNM patterns and inter-nodal metastatic correlations. Two optimized CTVn delineation recommendations for definitive concurrent chemoradiotherapy of LUAD and LUSC were proposed to enhance targeting precision.

1. Background

Lung cancer remains a leading global public health burden, accounting for over 1.8 million deaths worldwide in 2022, representing 18.7% of all cancer-related mortality[1]. In China, the incidence of lung cancer constitutes 22.0% of all malignancies, with a mortality rate as high as 28.5%—significantly exceeding the global average[2]. Lung adenocarcinoma (LUAD, of bronchial glandular origin) and lung squamous cell carcinoma (LUSC, of bronchial epithelial origin) are the two predominant subtypes of non-small-cell lung cancer (NSCLC), accounting for approximately 50% and 20–30% of cases, respectively[3,

4]. As is well-known, these two histological subtypes exhibit distinct pathological origins, clinicopathological features, and tumor biological behaviors[5].

Despite the advent of novel anticancer agents[6], concurrent or sequential chemoradiotherapy remains an irreplaceable treatment modality for locally advanced unresectable NSCLC[7,8]. The 2018 ESTRO ACROP consensus emphasized the indispensable role of radiotherapy and provided recommendations for target volume delineation[9]. Defining the clinical target volume (CTV) for lymph nodes requires a thorough understanding of LNM patterns; however, significant controversy persists regarding the biological LNM characteristics specific to LUAD and LUSC[10,11].

Involved-field irradiation (IFI) is currently recommended for locally advanced inoperable NSCLC instead of elective nodal irradiation (ENI); nonetheless, discrepancies remain regarding optimal CTV delineation for lymph nodes. Previous studies and major NSCLC CTV delineation guidelines recommend an 8 mm expansion margin for LUAD and 6 mm for LUSC to cover 95% of microscopic extension[12]. This recommendation acknowledges the difference in gross tumor microscopic extension between the two subtypes but fails to address disparities in regional nodal metastasis patterns or provide corresponding CTV margin recommendations. Furthermore, the core evidence supporting involved-field radiation therapy (IFRT) stems from retrospective studies reporting elective nodal failure (ENF) rates below 10%—defined as recurrence in initially uninvolved lymph nodes without local failure[13–15]. Critically, these studies pooled all NSCLC subtypes without stratifying ENF rates by histology (LUAD vs. LUSC) or providing subtype-specific analyses. Consequently, the risk of out-field failure in LUAD versus LUSC patients treated with IFRT remains unclear. More importantly, no prospective randomized head-to-head trials have compared the efficacy and safety of ENI versus IFRT in locally advanced unresectable NSCLC, particularly stratified by histological subtype.

Positron emission tomography-computed tomography (PET-CT) offers superior diagnostic accuracy and is strongly recommended by the ESTRO ACROP and IAEA guidelines as a core technique for target volume delineation in locally advanced NSCLC radiotherapy[16,17]. It is widely recognized as the most precise imaging modality for investigating regional LNM patterns in NSCLC, especially in unresectable locally advanced disease. Our team previously explored regional LNM patterns in locally advanced NSCLC using PET-CT imaging[18]; however, PET-CT inherently has false-positive and false-negative limitations, particularly in cases complicated by tuberculous infections, granulomatous benign lesions, or chronic inflammatory conditions[19]. Postoperative pathological data can serve as a confirmatory tool to improve diagnostic accuracy but is limited by the fact that patients undergoing radical surgery typically present at earlier stages[20]. Additionally, surgical pathology lacks comprehensive regional LNM information (e.g., contralateral mediastinal or supraclavicular nodes are rarely dissected intraoperatively), failing to fully reflect inherent LNM patterns—especially in locally advanced unresectable NSCLC. Therefore, a comprehensive systematic analysis integrating high-precision imaging and pathological data is essential to elucidate the inherent regional LNM patterns in NSCLC.

In this study, we further investigated differences in regional LNM patterns between LUAD and LUSC by integrating PET-CT imaging data and postoperative pathological findings. Our objectives were to: (1) identify consistent NSCLC LNM patterns validated by both modalities; (2) systematically characterize subtype-specific differences and inter-nodal metastatic correlations; and (3) provide evidence-based guidance for precise radiotherapy target delineation.

2. Methods

2.1 Patient Eligibility

We retrospectively enrolled 422 pathologically confirmed NSCLC patients (281 LUAD, 141 LUSC) who underwent PET-CT examinations at the General Hospital of Western Theater Command of PLA between January 2018 and August 2024. Postoperative pathology data were collected from 305 additional NSCLC patients (236 LUAD, 69 LUSC) who underwent radical surgical resection at the same institution between January 2017 and August 2024. Exclusion criteria included: (1) N0 stage disease; (2) prior antitumor therapy; (3) incomplete clinical data; (4) mixed NSCLC subtypes; and (5) secondary lung malignancies. All cases were staged according to the American Joint Committee on Cancer (AJCC)/Union for International Cancer Control (UICC) 8th edition TNM staging system. This study was approved by the Ethics Committee of the General Hospital of Western Theater Command of PLA (Approval No. : EC5-ky004), with a waiver of informed consent due to its retrospective nature.

2.2 Imaging Examination and LNM Confirmation

Lymph node mapping followed the 2009 International Association for the Study of Lung Cancer (IASLC) nodal classification. The PET-CT examination protocol and image interpretation criteria were consistent with our previously published methodology[18]. A lymph node was defined as metastatic on PET-CT if it met all the following criteria: (1) short-axis diameter ≥ 1.0 cm; (2) maximum standardized uptake value (SUVmax) ≥ 2.5; and (3) absence of plaque-like calcification. Lymph nodes enlarged on CT without significant radiotracer uptake were not considered metastatic.

For postoperative pathological specimens, the Ki-67 proliferation index was assessed by immunohistochemistry to quantify tumor cell nuclear positivity. Pathologists microscopically evaluated and documented vascular invasion, neural invasion, pleural involvement, and spread through air spaces (STAS). The maximum diameter of the primary tumor was measured intraoperatively and confirmed pathologically, then categorized according to T-stage criteria.

2.3 Statistical Analysis

Data were organized using Microsoft Excel and analyzed with IBM SPSS Statistics® 27 software. Categorical variables were presented as frequencies (percentages), with inter-group comparisons performed using the chi-square test or Fisher’s exact test (when expected frequencies < 5). Continuous variables conforming to a normal distribution (e.g., age, maximum tumor diameter) were expressed as mean ± standard deviation; non-normal variables were presented as median (interquartile range). Inter-

group comparisons of continuous variables were performed using the independent samples t-test or Mann-Whitney U test, as appropriate.

Binary logistic regression models were employed for multivariate analysis to explore correlations between metastatic lymph node levels. The Hosmer-Lemeshow test was used to assess logistic regression model goodness-of-fit, with a p-value > 0.05 indicating satisfactory model calibration. All tests were two-sided, with a p-value < 0.05 considered statistically significant.

3. Results

3.1 Baseline Patient Characteristics

The PET-CT cohort included 422 NSCLC patients (281 LUAD [66.6%], 141 LUSC [33.4%]). Baseline characteristics are detailed in Table 1. No significant differences were observed in age distribution or primary tumor location between subtypes. LUSC was associated with larger maximum tumor diameter (5.48 ± 2.53 cm vs. 3.87 ± 2.03 cm, p < 0.01) and lower distant metastasis rate (33.3% vs. 64.4%, p < 0.01) compared with LUAD. LUAD exhibited higher rates of lymph vascular invasion (62.3% vs. 47.8%, p = 0.032) and spread through air spaces (STAS; 21.6% vs. 5.8%, p = 0.003). The pathological cohort included 305 NSCLC patients (236 LUAD [77.4%], 69 LUSC [22.6%]). Baseline characteristics are presented in Table 2. No significant differences were noted in median age or overall lobar distribution. Statistically significant differences are highlighted in bold.

Table 1. Clinical Baseline Characteristics of LUAD and LUSC Based on PET-CT

Characteristic	LUAD, n=281(66.6%)	LUSC, n=141(33.4%)	*p* Value
Median age[year, M($P_{25,}$ P_{75})]	64(56,71)	65(58,71)	0.408
Gender			<0.001
Male	154(54.8%)	**125(88.7%)**	
Female	**127(45.2%)**	16(11.3%)	
Location of primary tumor			0.275
Left Lung	120(42.7%)	70(49.6%)	
Superior lobe	78(27.8%)	38(27.0%)	
Inferior lobe	42(14.9%)	32(22.6%)	
Right lung	161(57.3%)	71(50.4%)	
Superior lobe	79(28.1%)	31(22.0%)	
Middle lobe	19(6.8%)	7(5.0%)	
Inferior lobe	63(22.4%)	33(23.4%)	
Tumor type			<0.001
Peripheral lung cancer	**238(84.7%)**	53(37.6%)	
Central lung cancer	43(15.3%)	**88(62.4%)**	
Maximum diameter [cm,x±s]	3.87±2.03	**5.48±2.53**	<0.001
Local invasion	166(59.1%)	91(64.5%)	0.278
Visceral pleura	136(48.4%)	64(45.4%)	0.559
Mediastinum	29(10.3%)	21(14.9)	0.170
Separate nodules in same lobe	**51(18.1%)**	12(8.5%)	0.009
Separate nodules in different ipsilateral lobe	**49(17.3%)**	8(5.7%)	<0.001
Others	6(2.1%)	13(9.2%)	<0.001
N classification			0.208
N1	23(8.2%)	18(12.8%)	
N2	100(35.6%)	54(38.3%)	
N3	158(56.2%)	69(48.9%)	
Characteristic	LUAD,	LUSC,	*p* Value

	n=281(66.6%)	n=141(33.4%)	
T classification			0.196
T1a	1(0.4%)	0(0)	
T1b	34(12.1%)	5(3.5%)	
T1c	36(12.8%)	11(7.8%)	
T2a	58(20.6%)	25(20.6%)	
T2b	26(9.3%)	16(11.3%)	
T3	49(17.4%)	32(22.7%)	
T4	77(27.4%)	52(36.9%)	
M classification			<0.001
M0	100(35.6%)	**96(68.1%)**	
M1	**181(64.4%)**	45(31.9%)	
M1a	32(11.4%)	10(7.1%)	
M1b	**72(25.6%)**	16(11.3%)	
M1c	**77(27.4%)**	19(13.5%)	
TNM Stage			0.101
ⅡB	11(3.9%)	18(4.3%)	
ⅢA	33(11.7%)	59(14.0%)	
ⅢB	36(12.8%)	70(16.6%)	
ⅢC	20(7.1%)	49(11.6%)	
ⅣA	104(37%)	129(30.6%)	
ⅣB	77(27.4%)	97(23.0%)	
Distant metastasis	181(64.4%)	47(33.3%)	<0.001
Bone	128(45.6%)	24(17.0%)	<0.001
Pleural dissemination	49(17.4%)	15(10.6%)	0.066
Liver	24(8.5%)	9(6.4%)	0.436
Contralateral lung	**37(13.2%)**	7(5.0%)	0.009
Brain	**20(7.1%)**	2(1.4)	0.013
Adrenal gland	28(9.7%)	7(5.0%)	0.079

Table 2. Clinical Baseline Characteristics of LUAD and LUSC Based on Pathological Data

Characteristic	LUAD n=236 (77.4%)	LUSC n=69(22.6%)	*p* Value
Median age [year, M (P25, P75)]	56.5(25, 75)	58(IQR, 53-63)	0.232
Gender			<0.001
Male	119(50.4%)	**62(89.9%)**	
Female	**117(49.6%)**	7(10.1%)	
Location of primary tumor			0.328
Left Lung	86(36.4%)	29(42.0%)	0.399
Superior lobe	43(18.2%)	14(20.3%)	
Inferior lobe	43(18.2%)	15(21.7%)	
Right lung	150(63.6%)	40(58.0%)	0.399
Superior lobe	70(29.7%)	13(18.8%)	
Middle lobe	23(9.7%)	11(15.9%)	
Inferior lobe	57(24.2%)	16(23.2%)	
Maximum diameter [cm, M (P25, P75)]	2.50 (2.0, 3.5)	**3.20 (2.5, 3.0)**	**<0.001**
Pathological characteristics			
Visceral pleura	**158(66.9%)**	32(46.4%)	**0.002**
Neural invasion	55(23.3%)	10(14.5%)	0.116
Vascular invasion	**147(62.3%)**	33(47.8%)	**0.032**
Spread through air spaces	**61(21.6%)**	4(5.8%)	**0.003**
Bronchial stump	1(0.4%)	2(2.9%)	0.067
Ki-67 score			**<0.001**
Median score [M (P25, P75)]	20%(10%, 30%)	**40%(30%, 60%)**	
Range	2%-60%	3%-70%	
N classification			**0.019**
N1	59(25.0%)	29(42.0%)	
N2	**175(74.2%)**	40(58.0%)	
N3	2(2.8%)	0	

3.2 Concordance Between PET-CT and Pathological LNM Patterns

Overall, PET-CT and postoperative pathological data exhibited high concordance in LNM distribution patterns for both LUAD and LUSC, confirming the reliability of PET-CT-derived LNM patterns. For LUAD across pulmonary lobes, the top five metastatic nodal levels identified by both modalities showed substantial overlap: left superior lobe (10L, 5, 4L, 6); left inferior lobe (10L, 7, 4L, 5); right upper lobe (10R, 4R, 2R, 7); right middle lobe (10R, 7, 4R, 2R); and right inferior lobe (7, 10R, 4R, 2R). For LUSC across pulmonary lobes, concordant top metastatic levels included: left superior lobe (10L, 4L, 5, 7); left inferior lobe (10L, 7, 4L, 5); right upper lobe (10R, 4R, 2R, 7); right middle lobe (10R, 4R, 2R); and right inferior lobe (10R, 7, 4R, 2R) (Table 3).

Table 3
Comparative Analysis of Lobar LNM Distribution in LUAD vs. LUSC by Pulmonary Lobe Based on PET-CT and Postoperative Pathology Data

Characteristic	**LUAD n = 236 (77.4%)**	**LUSC n = 69(22.6%)**	***p* Value**
Median age [year, M (P25, P75)]	56.5(25, 75)	58(IQR, 53–63)	0.232
Gender			< 0.001
Male	119(50.4%)	**62(89.9%)**	
Female	**117(49.6%)**	7(10.1%)	
Location of primary tumor			0.328
Left Lung	86(36.4%)	29(42.0%)	0.399
Superior lobe	43(18.2%)	14(20.3%)	
Inferior lobe	43(18.2%)	15(21.7%)	
Right lung	150(63.6%)	40(58.0%)	0.399
Superior lobe	70(29.7%)	13(18.8%)	
Middle lobe	23(9.7%)	11(15.9%)	
Inferior lobe	57(24.2%)	16(23.2%)	
Maximum diameter [cm, M (P25, P75)]	2.50 (2.0, 3.5)	**3.20 (2.5, 3.0)**	**< 0.001**
Pathological characteristics			
Visceral pleura	**158(66.9%)**	32(46.4%)	**0.002**
Neural invasion	55(23.3%)	10(14.5%)	0.116
Vascular invasion	**147(62.3%)**	33(47.8%)	**0.032**
Spread through air spaces	**61(21.6%)**	4(5.8%)	**0.003**
Bronchial stump	1(0.4%)	2(2.9%)	0.067
Ki-67 score			**< 0.001**
Median score [M (P25, P75)]	20%(10%, 30%)	**40%(30%, 60%)**	
Range	2%-60%	3%-70%	
N classification			**0.019**
N1	59(25.0%)	29(42.0%)	
N2	**175(74.2%)**	40(58.0%)	
N3	2(2.8%)	0	

3.3 Subtype-Specific LNM Distribution Patterns

Pathological analysis of resectable NSCLC revealed distinct LNM distribution patterns between LUAD and LUSC (Figure S1, Table S1). Specifically, LUAD demonstrated a significantly higher metastasis rate at level 4R (29.2% vs. 13.0%, p = 0.007) and a trend toward increased level 2R involvement (25.0% vs. 14.5%, p = 0.067) compared with LUSC—particularly in the right lung (Tables S3, S4). Univariate and multivariate analyses identified inter-nodal metastatic correlations in resected LUAD: 2R metastasis correlated with ipsilateral 4R; 4L correlated with 6; and level 7 correlated with level 9 (Table S5). Limitations of surgical pathology included infrequent dissection of supraclavicular lymph nodes (SCLN) and inability to assess nodes outside the surgical field—gaps effectively addressed by PET-CT.

PET-CT analysis further confirmed subtype-specific LNM distributions (Figure S2, Table S2). As shown in Table 4, LUAD had higher SCLN metastasis rates (1L: 21.0% vs. 12.1%, p = 0.024; 1R: 31.7% vs. 19.9%, p = 0.011), while LUSC exhibited higher level 8 metastasis (29.8% vs. 19.9%, p = 0.024). Multivariate analysis revealed that LUAD conferred 1.87-fold (1R, 95%CI: 1.15–3.04) and 1.94-fold (1L, 95%CI: 1.08–3.47) increased SCLN metastasis risks compared with LUSC.

Table 4
Comparison of Overall LNM Rates Between LUAD and LUSC based on PET-CT data.

LNM Levels	The number and rate of LNM		*P* value
	LUAD (n = 281)	LUSC (n = 141)	
1L	**59(21.0%)**	**17(12.1%)**	**0.024**
1R	**89(31.7%)**	**28(19.9%)**	**0.011**
2L	36(12.8%)	12(8.5%)	0.189
2R	109(38.8%)	49(34.8%)	0.419
3a	42(14.9%)	21(14.9%)	0.989
3p	11(3.9%)	2(1.4%)	0.162
4L	116(41.3%)	60(42.6%)	0.803
4R	175(62.3%)	83(58.9%)	0.498
5	96(34.2%)	46(32.6%)	0.752
6	64(22.8%)	31(22.0%)	0.855
7	155(55.2%)	87(61.7%)	0.200
8	**56(19.9%)**	**42(29.8%)**	**0.024**
9	32(11.4%)	22(15.6%)	0.221
10L	112(39.9%)	64(45.4%)	0.277
10R	168(59.8%)	82(58.2%)	0.748
L-IPLN	43(15.3%)	26(18.4%)	0.411
R-IPLN	65(23.1%)	30(21.3%)	0.667

Side-stratified analysis showed that left lung LUSC had higher level 8 metastasis (38.6% vs. 18.3%, p = 0.002), while left lung LUAD had greater contralateral 1R involvement (24.2% vs. 10.0%, p = 0.016). For right lung tumors, LUAD exhibited increased contralateral 1L (17.4% vs. 7.0%, p = 0.038) and contralateral hilar 10L metastasis (10.6% vs. 2.8%, p = 0.048) (Table S6). Lobar-specific analysis demonstrated that left inferior lobe LUSC had higher level 8 metastasis (50.0% vs. 26.2%, p = 0.035), while right inferior lobe LUAD showed increased contralateral 1L (20.0% vs. 3.0%, p = 0.020) and 10L metastasis (11.0% vs. 0%, p = 0.047) (Tables S7, S8).

Employing the same method as resected LUAD data, we also explored potential relationships among metastatic lymph node levels. Specifically, for the LUAD patients, significant correlations were confirmed between level 1L and 1R, 3a, 4L and 6, as well as correlation between 1R and 1L, 2L, 2R and 10R.

Similarly, 2L was linked with 1R, 4L and 6, and 2R exhibited pronounced connections with 1R and 4R (both $p < 0.001$). Level 3a correlated with 1L and 6 (See Table S9).

3.4 High-Risk Factors for Site-Specific Metastasis

Given the identified propensity for SCLN metastasis in LUAD, we sought to characterize the high-risk patient to guide radiotherapy planning. LUAD patients with SCLN metastasis were compared with those without to identify high-risk features (Table 5). Multivariate analysis revealed that LUAD with mediastinal invasion (T3), ipsilateral multi-lobar separate nodules (T4), or LNM at levels 2L, 2R, 3a, or 6 had significantly higher SCLN metastasis risk (all $p < 0.05$). Comparison of LUSC patients with and without level 8 metastasis identified key risk factors (Table 6): left inferior lobe origin (38.1% vs. 16.2%, $p < 0.05$) and larger maximum tumor diameter (6.305 ± 2.744 cm vs. 5.129 ± 2.36 cm, $p = 0.011$) were independently associated with level 8 metastasis. Fisher's exact test was used for location analysis due to expected frequencies < 5 in 20% of cells.

Table 5
Comparasion of LUAD patients with/without supraclavicular lymph nodes metastasis

Characteristic	SCLNM (+) n = 110	SCLNM (-) n = 170	*p* Value
Local invasion			0.013
Visceral pleura	56(50.9%)	80(47.1%)	
Mediastinum	**15(13.6%)**	14(8.2%)	**< 0.05**
Separate nodules in same lobe (T3)	32(29.1%)	19(11.2%)	
Separate nodules in different ipsilateral lobe (T4)	**30(27.3%)**	19(11.2%)	**< 0.05**
Others	1(0.91%)	5(2.9%)	/
Lymph node metastasis			< 0.01
2L	**29(26.4%)**	7(4.1%)	**< 0.05**
2R	**76(69.1%)**	33(19.4%)	**< 0.05**
3a	**36(32.7%)**	6(3.5%)	**< 0.05**
3p	9(8.2%)	2(1.2%)	
4L	64(58.2%)	52(30.6%)	
4R	91(82.7%)	84(49.4%)	
5	47(42.7%)	49(28.8%)	
6	**48(43.6%)**	16(9.4%)	**< 0.05**
7	79(71.8%)	75(44.1%)	
8	33(30%)	23(13.5%)	
9	17(15.5%)	15(8.8%)	
10L	44(40%)	68(40%)	
10R	82(74.5%)	85(50%)	
L-IPLN	18(16.4%)	25(14.7%)	
R-IPLN	39(35.5%)	25(14.7%)	

Table 6
Comparison of LUSC patients with/without level 8 metastasis

Characteristic	Level 8 (+) n = 42	Level 8 (-) n = 99	*p* Value
Location of primary tumor			0.009*
Left Lung	27 (64.3%)	43 (43.4%)	
Superior lobe	11 (26.2%)	27 (27.3%)	
Inferior lobe	**16 (38.1%)**	16 (16.2%)	< 0.05
Right lung	15 (35.7%)	56 (56.6%)	
Superior lobe	4 (9.5%)	27 (27.3%)	< 0.05
Middle lobe	0	7 (7.1%)	
Inferior lobe	11 (26.2%)	22 (22.2%)	
Maximum diameter [cm, x ± s]	**6.305 ± 2.744**	5.129 ± 2.36	0.011

*: As the theoretical frequency was less than 5 in 20% of the data, the Fisher's exact test was employed for this analysis.

4. Discussion

Building on our prior work in *Radiation Oncology* demonstrating significant LNM correlations in inoperable NSCLC[18], this study integrated PET-CT data from 422 treatment-naive patients and pathological data from 305 surgical cases to investigate lobar-specific LNM patterns and inter-nodal correlations between LUAD and LUSC. Our findings confirm that LUAD exhibits a more aggressive metastatic phenotype and underscore fundamental differences in LNM patterns between subtypes—supporting histology-adapted CTV delineation to enhance radiotherapy precision.

Lobar-specific analyses revealed distinct metastatic signatures: LUAD primarily involved levels 5/10L/4L/6/7 in the left lung and 10R/2R/4R/7 in the right lung, with the highest metastasis rates in the right middle/lower lobes (particularly the right inferior lobe). In contrast, LUSC predominantly metastasized to levels 10L/7/4L in the left lung and 7/10R/4R/2R in the right lung.

CTV delineation in NSCLC radiotherapy remains heavily experience-dependent due to the paucity of prospective evidence. To some extent, our findings address this critical gap by providing subtype-specific data to be expected to optimize definitive radiotherapy planning (though prospective validation is still needed). The ESTRO ACROP guidelines recommend IFRT for locally advanced inoperable NSCLC and offer two CTV delineation options: Option 1 (inclusion of entire involved nodal stations with ≥ 5–8 mm margin around GTV) and Option 2 (geometric GTV-to-CTV expansion [5–8 mm] with smaller volume) [13–15]. Consistent with prior evidence of low out-field recurrence with IFRT, we advocate for IFRT over

ENI but propose subtype stratification: LUAD may benefit from Option 1 (larger volume) while LUSC is better suited for Option 2 (smaller volume).

The ESTRO ACROP guidelines also mention elective inclusion of hilar and/or neighboring nodal stations but do not define "neighboring" or specify inclusion criteria[21]. Our data partially clarify these ambiguities by identifying some subtype-specific high-risk stations such as SCLN for LUAD and level 8 for large-volume LUSC. Integrating these findings with guideline recommendations, we propose optimized CTVn delineation strategies for LUAD and LUSC (Table 7). Of course, future studies should specifically evaluate out-field failure rates by subtype and conduct prospective trials of subtype-adapted CTV delineation.

This study has several limitations. First, its retrospective design means our CTVn recommendations require prospective validation. Second, factors including tumor differentiation grade, central/peripheral location, and EGFR mutation status—potential modifiers of LNM patterns—were not analyzed (e.g., poorly differentiated LUSC may mimic LUAD behavior). Third, single-center enrollment introduces potential selection bias despite large sample sizes. Fourth, PET-CT false positives/negatives and unevaluated molecular features (EGFR/PD-L1) may limit interpretation. Future multicenter prospective studies should integrate clinical, imaging, and pathological data to refine LNM prediction models, explore molecular/subtype modifiers, and leverage radiomics/artificial intelligence to enhance detection accuracy.

Table 7
Suggestion for CTV delineation.

LUAD	LUSC
ESTRO ACROP guideline's Option 1 (lymph node stations): (1) inclusion of the whole pathologically affected lymph node station (Fig. 1a) including at least a 8 mm margin around the GTV. (2) Inclusion of the hilum and uninvolved areas between involved stations. (3) Inclusion of the neighbouring lymph node stations should be considered l as below.	ESTRO ACROP guideline's Option 2 (geometric expansion): (1) geometric expansion of nodal GTV to CTV in analogy to the primary tumour (5–8 mm) (Fig. 1b). (2) Inclusion of hilum station is optional. (3) Inclusion of uninvolved areas between involved stations (especially the hilum) is optional (4) Inclusion of the neighbouring lymph node stations should be considered as below.
Note: If the primary tumor directly invades the mediastinum, metastasizes to different lobes of the ipsilateral lung (T4) and metastasizes to lymph nodes in level of 2, 3a, and 6, it is recommended that CTVn include 1L/R on the same side or both sides.	**Note**: If the tumor is located in the left lower lobe especially for central-type lung cancer and tumor volume is large (≥ 6 cm in diameter), it is recommended that CTVn include level of 8.

5. Conclusions

By integrating PET-CT imaging and postoperative pathological data, this histology-stratified, lobar-specific analysis confirms distinct regional LNM patterns and inter-nodal correlations between LUAD and LUSC. The optimized CTVn delineation recommendations proposed for definitive concurrent

chemoradiotherapy of LUAD and LUSC provide a evidence-based framework to enhance targeting precision and personalize radiotherapy planning.

List of abbreviations

Abbreviations	Full Forms
LUAD	Lung adenocarcinoma
LUSC	Lung squamous cell carcinoma
NSCLC	Non-small-cell lung cancer
ESTRO ACROP	European Society for Radiotherapy & Oncology Advisory Committee on Radiation Oncology Practice
CTV	Clinical target volume
GTV	Gross tumor volume
LNM	Lymph node metastasis
IFI	Involved-field irradiation
ENI	Elective nodal irradiation
ENF	Elective nodal failure
IFRT	Involved-field radiation therapy
IAEA	International Atomic Energy Agency Guidelines
PET-CT	Positron emission tomography-computed tomography
AJCC	American Joint Committee on Cancer
UICC	Union for International Cancer Control
STAS	Spread through air spaces
SCLN	Supraclavicular lymph nodes

Declarations

Ethics approval and consent to participate

This study was conducted in accordance with the principles of the Declaration of Helsinki. The research protocol, including the waiver of informed consent, was reviewed and approved by the Ethics Committee of the General Hospital of Western Theater Command of PLA (Approval No.: EC5-ky004). Due to the retrospective nature of this study, which involved the analysis of existing anonymized data, the requirement for obtaining individual informed consent was formally waived by the aforementioned Ethics Committee.

Consent for publication

Not applicable.

Competing interests

The authors declare no known competing financial interests or personal relationships that could have appeared to influence the work reported in this paper.

Funding

Not applicable.

Author Contribution

Zheng Liu: Writing – Original Draft, Validation, Methodology, Investigation, Software, Formal Analysis; Xiaomei Qian:Data curation, Investigation; Zhihui Li:Methodology; Zhiming Chen: Validation, Resources; Guangjie Wang: Project administration, Resources; Feifan Sun: Software; Hui Gao: Investigation; Jingjing Peng: Methodology; Xiaoli Huang: Validation; Jianqiong Feng: Resources; Min Du: Supervision; Jing Xian: Validation; Lingbo Bao: Validation; Hong Luo: Validation; Binglin Tang: Supervision; Yiyang Hu: Supervision; Yi Li: Supervision; Chao Wang: Validation, Supervision; Chaoyang Jiang: Resources, Validation; Daijun Zhou: Conceptualization, Validation, Supervision; Dong Li: Conceptualization, Resources, Validation, Supervision, Project administration, Writing – Review & Editing.

Acknowledgement

The authors gratefully acknowledge the staff of the Department of Oncology and Department of Nuclear Medicine at the General Hospital of Western Theater Command for their assistance with data collection.

Data Availability

The data are available from the corresponding author on reasonable request.

References

1. Bray F, Laversanne M, Sung H, et al. Global cancer statistics 2022: GLOBOCAN estimates of incidence and mortality worldwide for 36 cancers in 185 countries. *CA: A Cancer Journal for Clinicians*. 2024;74:229-263.

2. Han B, Zheng R, Zeng H, et al. Cancer incidence and mortality in China, 2022. *Journal of the National Cancer Center*. 2024;4:47-53.
3. Nicholson AG, Tsao MS, Beasley MB, et al. The 2021 WHO Classification of Lung Tumors: Impact of Advances Since 2015. *Journal of Thoracic Oncology*. 2022;17:362-387.
4. Barta JA, Powell CA, Wisnivesky JP. Global Epidemiology of Lung Cancer. *Annals of Global Health*. 2019;85:1-11.
5. Relli V, Trerotola M, Guerra E, Alberti S. Abandoning the Notion of Non-Small Cell Lung Cancer. *Trends in Molecular Medicine*. 2019;25:585-594.
6. Li, H., Yuan, S., Wu, H., et al. Combination therapy using low-dose anlotinib and immune checkpoint inhibitors for extensive-stage small cell lung cancer. Cancer innovation, 3(6), e155.
7. Zhou Q, Chen M, Jiang O, et al. Sugemalimab versus placebo after concurrent or sequential chemoradiotherapy in patients with locally advanced, unresectable, stage III non-small-cell lung cancer in China (GEMSTONE-301): interim results of a randomised, double-blind, multicentre, phase 3 trial. *The Lancet Oncology*. 2022;23:209-219.
8. Xu Z, Zou Z, Hao X, et al. Adjuvant and neo-adjuvant immunotherapy in resectable non-small cell lung cancer (NSCLC): Current status and perspectives. Cancer innovation, 2(1), 65–78.
9. Nestle U, De Ruysscher D, Ricardi U, et al. ESTRO ACROP guidelines for target volume definition in the treatment of locally advanced non-small cell lung cancer. *Radiotherapy and Oncology*. 2018;127:1-5.
10. Kawase A, Yoshida J, Ishii G, et al. Differences between squamous cell carcinoma and adenocarcinoma of the lung: are adenocarcinoma and squamous cell carcinoma prognostically equal? *Japanese Journal of Clinical Oncology*. 2012;42:189-195.
11. Deng HY, Zeng M, Li G, et al. Lung Adenocarcinoma has a Higher Risk of Lymph Node Metastasis than Squamous Cell Carcinoma: A Propensity Score-Matched Analysis. *World Journal of Surgery*. 2019;43:955-962.
12. Giraud P, Antoine M, Larrouy A, et al. Evaluation of microscopic tumor extension in non-small-cell lung cancer for three-dimensional conformal radiotherapy planning. *International Journal of Radiation Oncology, Biology, Physics*. 2000;48:1015-1024.
13. Sulman EP, Komaki R, Klopp AH, et al. Exclusion of elective nodal irradiation is associated with minimal elective nodal failure in non-small cell lung cancer. *Radiation Oncology*. 2009;4:5.
14. Rosenzweig KE, Sim SE, Mychalczak B, et al. Elective nodal irradiation in the treatment of non-small-cell lung cancer with three-dimensional conformal radiation therapy. *International Journal of Radiation Oncology, Biology, Physics*. 2001;50:681-685.
15. Rosenzweig KE, Sura S, Jackson A, Yorke E. Involved-field radiation therapy for inoperable non small-cell lung cancer. *Journal of Clinical Oncology*. 2007;25:5557-5561.
16. Nestle U, Le Pechoux C, De Ruysscher D. Evolving target volume concepts in locally advanced non small cell lung cancer. *Translational Lung Cancer Research*. 2021;10:1999-2010.

17. Konert T, Vogel W, MacManus MP, et al. PET/CT imaging for target volume delineation in curative intent radiotherapy of non small cell lung cancer: IAEA consensus report 2014. *Radiotherapy and Oncology*. 2015;116:27-34.
18. Sun F, Chen Z, Zhou D, et al. Regularity and correlation analysis of regional lymph node metastasis in nonoperative patients with non-small cell lung cancer based on positron emission tomography/computed tomography images. *Radiation Oncology*. 2024;19:137.
19. Xu N, Wang M, Zhu Z, et al. Integrated positron emission tomography and computed tomography in preoperative lymph node staging of non-small cell lung cancer. *Chinese Medical Journal*. 2014;127:607-613.
20. Wang YX, Li BS, Huang W, et al. Pattern of lymph node metastases and its implication in radiotherapeutic clinical target volume in patients with non-small-cell lung cancer: a study of 2062 cases. The British journal of radiology. 2015;88(1056):20140288.
21. Nestle U, De Ruysscher D, Ricardi U, et al. ESTRO ACROP guidelines for target volume definition in the treatment of locally advanced non-small cell lung cancer. Radiother Oncol. 2018;127(1):1-5.

Figures

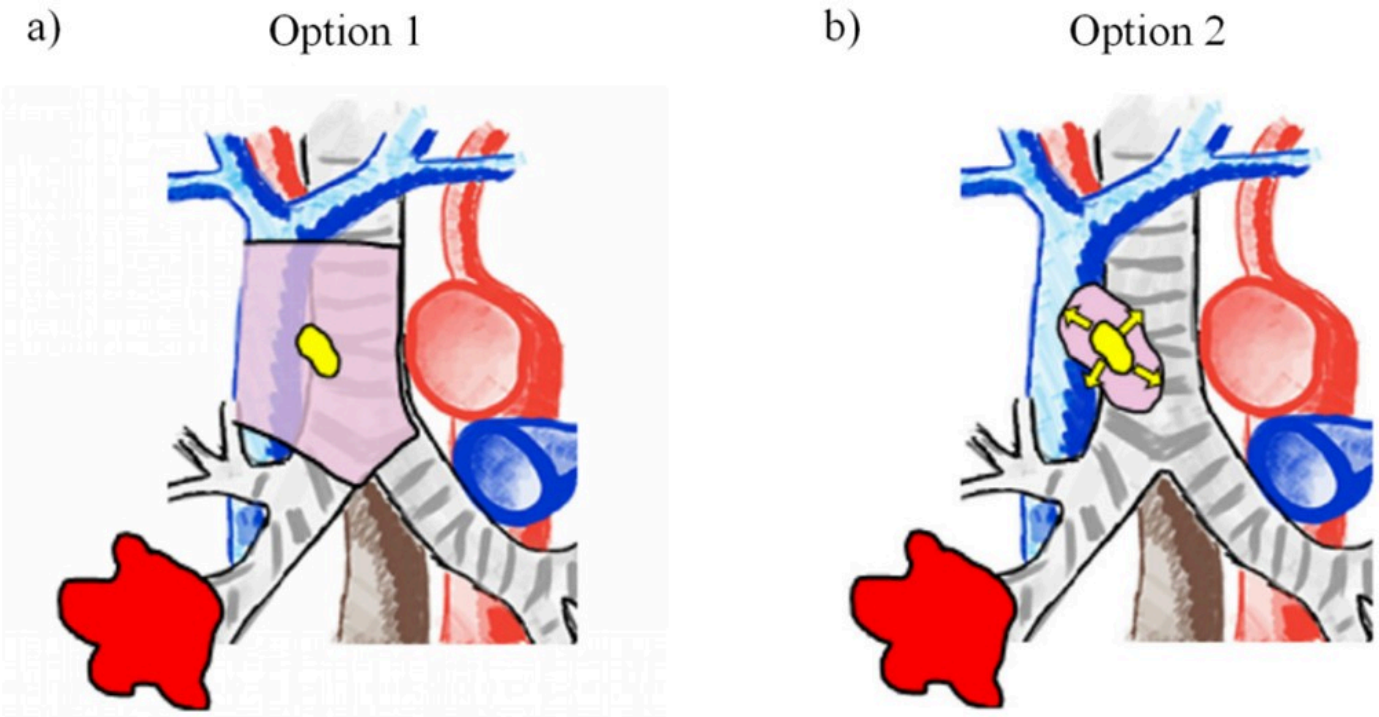

Figure 1

a) Option 1: CTV including the whole pathologically affected lymph node station. b) Option 2: Geometric expansion of nodal GTV to CTV in analogy to the primary tumor (5-8 mm) [21].

Supplementary Files

This is a list of supplementary files associated with this preprint. Click to download.

- supplementaryfiguresandtables.docx